Environmental Science Nano

Effects of Surface Coating Properties on the Sorption and Dissolution of ZnO Nanoparticles in Soil

Journal:	*Environmental Science: Nano*
Manuscript ID	EN-ART-03-2019-000348.R1
Article Type:	Paper
Date Submitted by the Author:	10-Jun-2019
Complete List of Authors:	Elhaj Baddar, Zeinah; University of Kentucky, Entomology Matocha, Chris; University of Kentucky, Plant and Soil Sciences Unrine, Jason; University of Kentucky,

Environmental Significance Statement

Manufactured nanomaterial fertilizers with coatings tuned to make them highly targeted are being explored for use in agriculture. Little is known about how coating properties influence nanomaterial behavior in soil. Using ZnO as a model nanofertilizer, we found that nanomaterial coatings influence stability, dissolution, and partitioning of nanomaterials to soil pore water. However, the properties of the "as synthesized" materials only partially explain their behavior. Affinity for natural organic matter must be considered when predicting the fate of coated ZnO nanomaterials in soil.

Environmental Science: Nano

ARTICLE

Surface Coating Effects on the Sorption and Dissolution of ZnO Nanoparticles in Soil

Zeinah Elhaj Baddar, Chris J. Matocha, and Jason M. Unrine *

Received 00th January 20xx,
Accepted 00th January 20xx

DOI: 10.1039/x0xx00000x

www.rsc.org/

Soil pH and dissolved organic matter (DOM) content are among the most important factors affecting the bioavailability of Zn and the binding and dissolution of ZnO nanoparticles (NPs). To investigated the effect of NP surface chemistry and DOM on the behavior of ZnO NPs and $ZnSO_4$ in soil solution at pH 6 and 8, we synthesized electrostatically stabilized (bare positively charged ZnO, and negatively charged (ZnO-$Zn_3(PO_4)_2$ core-shell NPs), and sterically and electrosterically stabilized (neutral dextran (DEX), and negatively charged dextran sulfate (DEX(SO_4))-ZnO NPs, respectively. We hypothesized that negatively charged ZnO NPs will have higher total Zn concentrations as opposed to neutral and positively charged ones in soil pore water at higher pH, with higher dissolution of the NPs at lower pH. At pH 8, core-shell and DEX-ZnO NP amendments had significantly higher total Zn concentration than $ZnSO_4$. To investigate the unexpected behavior of the neutral DEX-ZnO NPs, we performed sorption isotherm experiments which showed that DEX-ZnO NPs had the highest affinity for DOM of all ZnO NPs, which likely enhanced their colloidal stability and partitioning in soil pore water, especially at pH 8. In simple aqueous solution, with increasing ionic strength, negatively charged core-shell and DEX(SO_4) ZnO NPs were the most stable against aggregation. When DOM was introduced in to the system, the as-synthesized surface chemistry of the particles was altered, and all NPs became negatively charged. Dissolved Zn concentrations in soil extracts of NP amendments were similar while $ZnSO_4$ amended soils had the highest dissolved Zn among all treatments.

Introduction

There is an increasing interest in the use of nanoparticles (NPs) for delivery of agrochemicals such as micronutrients and pesticides(1). One application under investigation has been the use of ZnO NPs as micronutrient fertilizers. A few studies have reported significant increases in yields and tissue Zn concentrations in peanuts (*Arachis hypogaea*)(2), maize (*Zea mays*)(3), and sorghum (*Sorghum bicolor*)(4) when bare ZnO NPs were added as soil amendments. Even when applied at a concentration that was ten times lower than that of $ZnSO_4$, foliar application of chitosan coated ZnO NPs at 40 mg L^{-1} enhanced wheat (*Triticum aestivum*) grain Zn concentration by 30% as compared to a 50% increase achieved with $ZnSO_4$ at 400 mg L^{-1} (5).

In general, total metal concentration is a poor indicator of Zn bioavailability(6). Zinc bioavailability for plant uptake is limited by high soil pH, low geogenic Zn levels and high contents of phosphates, clay, natural organic matter (NOM), and carbonates(7). Therefore, using soluble Zn salts as fertilizers is often of limited success under these conditions. Likewise, soil properties may affect the bioavailability, fate, and behavior of ZnO NPs. Thus, the partitioning of nanoparticles to the soil pore water is an important determinant of the mobility and bioavailability of these nanoparticles for plant uptake.

Soil pH has a tremendous effect on the behavior of Zn ions. Higher soil pH is often associated with restricted bioavailability of nutrients, including Zn. The increase in soil pH is accompanied by the deprotonation of hydroxyl groups present on soil components such as clay aluminosilicates, Al/Fe oxohydroxides, or organic ligands, leading to the retention of Zn ions(8-10). Moreover, high soil pH induces Zn ion precipitation as poorly soluble Zn minerals (e.g. Zn carbonates, phosphates, and hydroxides)(10). On the other hand, lower soil pH enhances the bioavailability of Zn by solubilizing Zn complexes, in addition to the desorption from the now more protonated exchange sites on soil colloid surfaces.

Nanoparticle behavior is also dramatically affected by soil pH If the pH in a medium approaches the point of zero charge PZC (the

Department of Plant and Soil Sciences, University of Kentucky, Lexington, Kentucky 40546, United States. Email: jason.unrine@uky.edu

Electronic Supplementary Information (ESI) available: [details of any supplementary information available should be included here]. See DOI: 10.1039/x0xx00000x

pH at which positive and negative surface charges are balanced, resulting in an electrophoretic mobility of zero(11)), the particles will have a greater tendency to aggregate(12). On the other hand, at a pH higher than the PZC, particle surfaces will be more negatively charged, conferring a higher NP colloidal stability in the soil solution as they will most likely be repelled from negatively charged colloids in the soil, thus enhancing their partitioning to the soil solution. For bare ZnO NPs the PZC is about 9.3, giving them a net positive charge at most likely soil pH values. Solubility of ZnO is also strongly pH dependent. Solubility in water begins to increase below a pH of 7.3. Previous work has shown that low soil pH enhances the dissolution of ZnO NPs and results in an increase in Zn ion concentration(13-19).

Ionic strength also affects the NP colloidal stability. When electrolyte concentration increases, the electric double layer is compressed due to charge screening, which reduces the separation distances between particles and allows attractive forces to dominate, inducing aggregation. One study reported that the propensity of Ag NPs to aggregate in an electrolyte solution was found to be dependent on their surface chemistry, specifically organic coatings, according to the following order: bare Ag NPs > Ag NPs sterically stabilized with polyvinylpyrrolidone (PVP)> Ag NPs electrosterically stabilized with gum arabic (GA)(20).

Modification of NP surface chemistry by adding coatings is often implemented to impart colloidal stability and minimize aggregation(21). The initial surface chemistry of the as-synthesized particles can be dramatically altered in complex environmental media due to the loss of coating and/or replacement with natural organic material(22, 23). Dissolved organic matter can overcoat or replace original coatings on NP surfaces(24, 25). Due to the low pKa values of carboxylate functional groups, humic acids (HA) tend to have a negative charge under environmentally relevant conditions. Thus, whether DOM replaces or overcoats existing coatings, a negative charge will be imparted to these NPs, potentially enhancing their colloidal stability in soil solution. On the other hand, DOM could also induce NP dissolution due to the ligands exchange which occurs on the surface of these NPs(26).

This study investigated the effect of ZnO NP surface chemistry on their partitioning in soil pore water. According to the classical Derjaugin–Landau–Verwey–Overbeek (DLVO) theory, the interplay between attractive (Van der Waals) and repulsive (electrostatic) forces determines the aggregation status of colloids(27). Coatings can increase particle stability by increasing electrostatic or steric repulsion. Electrostatic stabilization involves imparting a charge to the particle surface to enhance their electrostatic repulsion. Steric stabilization is caused by osmotic constraints due to the conformation of macromolecules on two particle surfaces as they come into close proximity , thus increasing particle repulsion(28). Electrosteric stabilization combines both effects to further enhance particle stability against aggregation. In order to enhance NP resistance against aggregation, we stabilized bare ZnO NPs sterically through adding a nonionic coating (dextran), electrosterically through adding a polyelectrolyte (dextran sulfate) coating, and electrostatically by forming a shell of $Zn_3(PO_4)_2$ on a core of ZnO NPs. We will refer to these particles as: DEX, DEX(SO_4), and core-shell ZnO NPs hereafter. Core-shell and DEX(SO_4) ZnO NPs are negatively charged, therefore, we hypothesized that this would likely enhance their partitioning to the soil solution in comparison with the positively charged bare ZnO and the neutral DEX-ZnO NPs, especially under alkaline conditions. We expected DEX-ZnO NPs to initially bind to soil particles, as it has been shown that particles coated with neutral polymers have a high affinity for surfaces which are not coated with a like polymer(29). We also expected that acidic soil pH will induce the dissolution of ZnO NPs regardless of their surface chemistry.

Materials and Methods

Zinc Oxide Nanoparticles

A detailed description of synthesis protocols and characterization of ZnO NPs can be found in our previous work. In brief, alkaline precipitation in water was used to produce bare ZnO NPs. The aging of these NPs in phosphate solution under certain conditions leads to the formation of a core made of ZnO NPs that is covered by a shell of amorphous $Zn_3(PO_4)_2$(30). The addition of nonionic (dextran) and polyelectrolyte (dextran (SO_4)) of 9-15 kDa at 1:6 and 1:4 coating to Zn mass ratio during the synthesis resulted in the formation of DEX and DEX(SO_4) ZnO NPs, respectively.

Transmission electron microscopy (TEM), X-ray diffraction (XRD), dynamic light scattering (DLS), phase analysis light scattering (PALS), and thermogravimetric analysis (TGA) were used to determine, the primary particle size and shape, chemical form, hydrodynamic diameter, electrophoretic mobility, and the mass of coating on the particles, respectively. We also determined the PZC of these NPs by measuring the electrophoretic mobility of 100 mg Zn L^{-1} ZnO NPs suspensions at different pH values upon titrating with either HCl or NaOH.

Stability of ZnO Nanoparticles as a Function of Ionic Strength

To test the effect of ionic strength on the stability of ZnO NPs, suspensions of bare and coated particles were prepared at 500 mg Zn L^{-1} in DI using cup horn sonication (Qsonica, Newtown, Connecticut, USA) at 100% amplitude for 45 minutes at 225 W. Then 0.26 mL of each NP suspension was aliquoted in a 2 mL microcentrifuge tube, where 1.04 mL of 0, 1, 10, and 100 mM NaCl solutions were added to achieve a final concentration of 100 mg Zn L^{-1}. Hydrodynamic diameters and electrophoretic mobilities were measured using Zetasizer. We included DI water (0 mM) for comparison purposes since many studies use DI water, but it should be noted that differential dissolution of metal oxide particles can cause variation in ionic strength and pH in DI water.

Effect of pH and DOC on Zeta (ζ) Potential and Dissolution of ZnO Nanoparticles in Solution

We performed saturated paste extractions(31) from an unamended Sadler soil at both pH 6 and pH 8. The collected extracts were centrifuged for 4 hours at 16,837 x g (using a particle density of 2.67 g cm^{-3} for soil particles to obtain a size cut off of 35 nm diameter according to Stoke's law). The supernatants were aliquoted and referred to as particle free soil solution (PFSS) hereafter. To buffer the soil solution pH values, which decreased due to equilibration with the atmosphere, we added 2-(N-morpholino) ethanesulfonic acid (MES) and tris (hydroxymethyl) aminomethane (TRIS) buffers at a final concentration of 1 mM to achieve pH values of 6 and 8, respectively.

Zinc oxide NP suspensions were prepared at a nominal concentration of 250 mg L^{-1} Zn in DI water. Cup horn sonication for 45 minutes at 100% amplitude was used to disperse the NPs. In a 2 mL microcentrifuge tube, 0.12 mL of each ZnO NP suspension and DI water (Zn free control) were added to 1.15 mL PFSS at either pH 6 or pH 8 to achieve a final concentration of 25 mg Zn L^{-1}. Three replicates of each treatment were prepared. Sample pH values were measured prior to and after 24 h mixing at room temperature on a sample rotator that was set at maximum speed. Electrophoretic mobilities were measured after 24 h using phase

analysis light scattering (PALS; zetasizer nanoZS, Malvern Instruments, Malvern, United Kingdom). Particle ζ potential was estimated from electrophoretic mobilities using the Smoluchowski's approximation. These samples were then centrifuged for 3 hours at 16,837 X g, then a 0.5 mL aliquot of the supernatant was acidified to 0.16 M HNO_3 to measure the dissolved Zn in the PFSS using ICP-MS.

To address the effect of dissolved organic matter on the ζ potential of ZnO NPs, we added PPHA at a concentration of either 25 or 100 mg C L^{-1} to a 25 mg Zn L^{-1} suspension of each ZnO NP treatment in either PFSS, DI water, or MHRW. Dissolved C concentrations in our soils were as high as 125 and 237 mg C/L in the saturated paste extracts at pH 6 and 8, respectively (Table S2). Samples were left on a tube rotator as mentioned above. Sample pH was measured in all suspensions at each C concentration level (in DI water and MHRW), and in the PFSS at both pH levels. Particle ζ potential and dissolution were determined as described above.

Dissolved Organic Carbon Sorption Experiments

We performed batch experiments to discern the sorption of DOC on to the surface of the different ZnO NPs. Pahokee peat humic acid (PPHA) (International Humic Substances Society, IHSS, 1S103H) was used as the model DOC source. We dissolved 10 mg of PPHA in 100 mL DI water. The pH of the solution was brought up to 9 using 0.1M NaOH to facilitate dissolution. The solution was left to stir overnight at room temperature (22°C) and then filtered with a 0.2 μm nylon filter, and stored at 4°C. The DOC concentration in PPHA stock solution was 43 mg C L^{-1} as determined using a carbon analyser.

Zinc oxide NP suspensions at 1000 mg Zn L^{-1} were sonicated for 45 minutes at 100% amplitude. Moderately hard reconstituted water (MHRW) was prepared according to EPA method 600/4-90/027F(32). Briefly, in 1L DI water, the following salts were added to achieve the following measured concentrations, in g L^{-1}: 0.067, 0.123, 0.096, and 0.004 of $CaSO_4.2H_2O$, $MgSO_4.7H_2O$, $NaHCO_3$, and KCl, respectively. The pH of MHRW was adjusted to 8 throughout the sorption experiments to match the pH of PFSS which was 8. Batch experiments were carried out at room temperature (~ 22°C) in 15 mL metal free centrifuge tubes where 2 mL of MHRW was added to 0.8 mL ZnO NPs at a Zn concentration of 1000 mg Zn L^{-1} (final Zn concentration was 100 mg Zn L^{-1}). Serial dilution of PPHA stock solution was done as the volume was brought up to 8 mL using DI water. All suspensions were prepared in triplicate and incubated for 24 h on a sample rotator set at full speed to establish equilibrium. We previously determined that equilibrium was obtained in 24 hours in a separate experiment (Fig. S.2). The suspensions were then centrifuged for 3 h at 16,837 x g to obtain non-sorbed DOC.

To determine free dissolved organic carbon concentration, 75 μL were withdrawn from the supernatants and aliquoted into a 96 well plate, and a microplate reader was used to measure the absorbance at 254 nm(33, 34). We determined the molar extinction coefficient at 254 nm using the DOC concentration of the stock solution measured using a carbon analyzer ((TOC-V_{CPN} total carbon analyzer, Shimadzu Corporation, Columbia, MD, USA).

The plots of the free DOC concentration (C_e), in mg C L^{-1}, against sorbed DOC (q_e) in mg kg^{-1} best fit a Freundlich isotherm model, which is described by the following formula:

$$q_e = k_f C_e^{(1/n)} \quad (1)$$

where q_e is the amount of PPHA (mg C) adsorbed per unit mass of ZnO NP (g) at equilibrium, C_e is the concentration of free PPHA (mg C L^{-1}) at equilibrium, n is the linearity parameter, and k_f is the Freundlich coefficient which describes the binding affinity of PPHA to the surface of the particles.

The linearization approach was used to determine the Freundlich isotherm equation parameters, for each treatment where both (C_e) and (q_e) were log-transformed. Then, log(C_e) values were plotted against log(q_e) values. Linear regression was used to fit the data points. Slope and intercept in each regression represented (1/n) and k_f, respectively. These parameters were then used to plot the data points according to the Freundlich model.

Soil Characterization

Surface Sadler silt loam (fine-silty, mixed, mesic Fragiudalf) surface soil was obtained from The University of Kentucky Research and Education Centre at Princeton (KY, USA). The soil was air dried, ground, and sieved (<2mm). Chemical and physical characterization of the soil included the determination of pH in a 1:1 ratio of soil to 18MΩ DI water or 1M KCl(35), particle size distribution (texture) by hydrometer(36), and total organic C and N by Dumas combustion (1112 Series NC soil analyzer, Thermo Electronic Corporation, Waltham, MA, USA)(37). A factor of 1.724 was multiplied by the TOC value to convert soil TOC into organic matter content(37). Acid extractable major cations and trace metals were determined following EPA method 3052(38). We placed 0.25g soil and 10 mL concentrated nitric acid in Teflon bombs. Closed vessel microwave digestion (MARS Express microwave reaction system (CEM, Matthews, NC) was performed and the digestates were further diluted before measuring major cation and trace metal concentrations. Major cation concentrations were measured using inductively coupled plasma-optical emission spectrometry (ICP-OES, Vista Pro Simultaneous ICP-OES, Varian, Palo Alto, CA, USA). Trace metal concentrations were measured using Inductively coupled plasma mass spectrometry (ICP-MS, Agilent 7500cx Santa Clara, CA, USA). Major anions were extracted from the soil with water according to the method described by Judy et al. (39). Analysis of recovered anions from soil samples was performed using ion chromatography (ICS-3000, Dionex, Sunnyvale, CA, USA). Colorimetric methods; molybdate blue-stannous chloride(37) and indophenol blue(40),were used to determine total phosphorous and ammonium concentrations, respectively, in soil. Soil water holding capacity (WHC) was determined using pressure plate extractor (Soil Moisture Equipment Corp., Santa Barbra, CA, USA)(41). A Mehlich III extraction was used to estimate the bioavailable Zn fraction in soil(42).

Soil Spiking

In a 150 mL capacity disposable plastic beaker, 50 grams of air-dried soil were thoroughly mixed by a wooden stick with either 40 or 54 mg of $MgCO_3$ or MgO to increase soil pH to 6 and 8, respectively. The carbonates and oxide of Mg were chosen because, due to their relative acid neutralizing capacities, we could add similar amounts of Mg to each treatment. We chose to use $MgCO_3$ and MgO instead of Na_2CO_3 and NaOH because Na^+ acts as a dispersing agent and disrupts the soil structure, dispersing a large quantity of soil colloids. Given that we were investigating colloidal stability of ZnO NPs, we didn't want to cause conditions that would artificially increase colloid dispersal. We also avoided using $CaCO_3$ or CaO due to the tendency for Ca^{2+} to cause aggregation of colloids. Magnesium ions cause less aggregation than Ca^{2+} especially in the presence of dissolved organic matter(43). To achieve 30% WHC, 5 mL of DI water were added to each soil sample. After thorough mixing, the beakers were weighed and

covered with parafilm perforated by a few holes to allow air exchange.

Soil samples were left to equilibrate to the desired pH for 7d in an incubator at 15°C. At the end of the incubation period, masses were checked, and DI water was added as needed to compensate for evaporation. Zinc oxide NP suspensions of 1000 mg Zn L^{-1} were prepared by adding a known mass of NP powder to 5 mL DI water in a 15 mL centrifuge tube. The suspensions were sonicated using a cup horn sonicator at 100% amplitude for 45 minutes. The suspensions were then added to the soil samples and mixed thoroughly with a wooden stick, which also raised the moisture content to 60% WHC. The beakers were covered with parafilm with several holes to allow air exchange and were kept in the incubator at the same temperature for two more weeks. The masses of beakers were recorded, and DI water was added as needed to replace water lost during the incubation period, once every week. The experiment was terminated after 14 d of incubation.

Saturated Paste Extraction

In order to minimize dissolution and colloidal dispersion artefacts from using large ratios of water to soil, while still obtaining sufficient soil water for analysis, we prepared saturated pastes for extraction of total and dissolved Zn using standard methods(37). Hyperbaric filtration (Fann instrument company, Houston, TX, USA) was used to extract soil solution from the saturated paste. We used Ahlstrom 10 μm pore size filters. Saturated pastes were transferred to the filter unit and 600 kPa pressure was applied using air. The soil solution was collected and kept at 4°C. Recovery of Zn NPs or Zn ions through the filters ranged from 99-104%. Greater than 90% of 1 μm polystyrene/latex beads passed through the filters.

Total Zn in Spiked Soil and Total and Dissolved Zn in Saturated Paste Extracts

Total Zn concentrations were determined in soils prior to and after extracting the soil solution. Around 2.0 g of soil was dried to constant weight in the oven at 105 °C. Dried soil was ground, and 0.25 g were digested with concentrated HNO_3 as mentioned above using EPA method 3052(38).

Saturated paste extracts were vortexed for 30 seconds and 1mL was transferred to a 15 mL tube. Then, 0.75 mL of concentrated HNO_3 was added to each tube and an open vessel microwave digestion was performed according to EPA method 3005 A(44). The Zn concentration in these samples is defined as total Zn. Another 2 mL fraction of the extracted soil solution was centrifuged at 16,837 X g for 3 hours to eliminate particles of >7 nm diameter as calculated using Stoke's law. A one mL aliquot of supernatant was subsequently acidified to 0.16 M HNO_3. We defined this Zn fraction as the dissolved Zn. Total Zn concentrations were measured using inductively coupled plasma mass spectrometry following U.S. EPA method 200.8(45). Quality controls included use of digestion blanks, spike recovery, duplicates, initial calibration verification/continued calibration verification, and standard reference materials (Standard reference material 2710, Montana soil I, National Institute of Standards and Technology, Gaithersburg, MD, USA). Data were only accepted if the recovery of Zn from NIST 2710 was 75-100%, spike recovery was 85-105%, and the relative percent difference between dilution replicates was <10%.

Statistical Analysis

Hydrodynamic size and the electrophoretic mobility data in the electrolyte solutions followed ANOVA assumptions of normality and variance homogeneity. Therefore, we performed ANOVA, followed by Dunnett's test to examine the effect of electrolyte concentration on the hydrodynamic size and the electrophoretic mobility for each ZnO NP treatment separately. Electrophoretic mobility and dissolution data in PFSS, DI and MHRW followed the ANOVA assumptions and were analysed in a similar manner, where, the Tukey HSD multiple comparisons test was performed between different ZnO coatings at each PFSS soil pH or DOM concentration. Evaluation of total and dissolved Zn concentration in saturated paste extracts was performed with a randomized complete block design, where at each pH level each Zn treatment was replicated three times within each experimental block. There were two experimental blocks performed on different days. We used Proc GLM to test for significant main effects and 2 -way interactions at $\alpha = 0.05$. Multiple comparisons between treatments within statistically significant interaction or main effects were performed using Tukey's HSD adjustment (SAS 9.4, SAS Institute, Cary, NC).

Results

Zinc Oxide Nanoparticle Characterization

Detailed characterization of the ZnO NPs can be found in our previous work(46). Transmission electron micrographs (Fig. 1) showed that the particles were nearly spherical. The primary particle sizes were 24 ± 1, 27 ± 0.3, 18 ± 1, and 20 ± 1 nm (mean ± one standard deviation) for bare, core-shell, DEX, and DEX(SO_4) ZnO NPs, respectively. Intensity weighted hydrodynamic diameters were: 314 ± 32.8, 532 ± 44.6, 755 ± 191.8, and 304 ± 36.2 for bare, core-shell, DEX, and DEX(SO_4) - ZnO NPs, respectively.

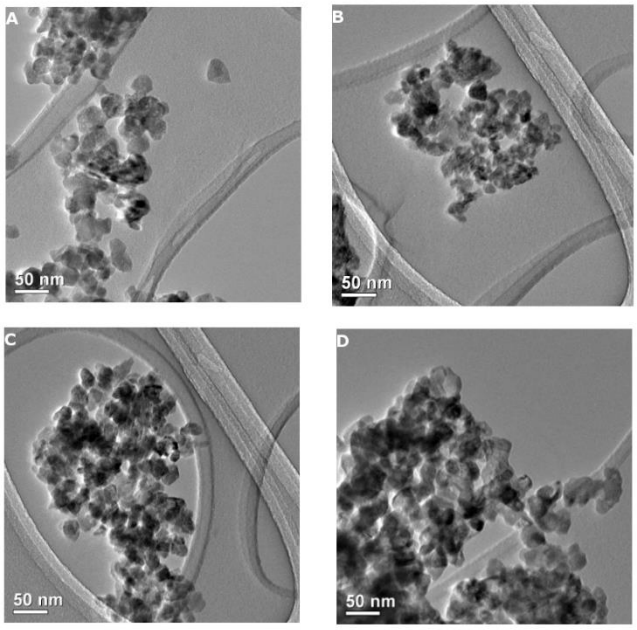

Fig. 1 Transmission electron micrographs of bare ZnO NPs (A), DEX - ZnO NPs (B), DEX (SO4)-ZnO NPs (C), ZnO-Zn3(PO4)2 core-shell NPs (D). Scale bar is 50 nm

Smoluchowski's approximation was used to calculate ζ potential values from electrophoretic mobilities measured in DI water, which were positive for the bare and DEX-ZnO NPs (29.1 ± 0.6 and 19.5 ± 1.1 mV) and negative for DEX(SO_4) and core-shell ZnO NPs (-24.8 ± 0.4 and -23.9 ± 2.3 mV). Point of zero charge values were determined graphically by plotting zeta potential values across a range of pH values (Fig. S3).Bare ZnO and DEX-ZnO NPs had higher PZC than DEX(SO_4) and core-shell ZnO NPs, where the former two had PZC values of 9.8 and 8.7, respectively, and the latter two had PZC values less than 6.2.

Diffractogram of powder XRD analysis of bare ZnO NPs can be found in our previous work(46), while the rest of ZnO NP diffractograms can be found in the supplementary information (Fig. S 1)

Effect of Ionic Strength on Hydrodynamic Diameter and Zeta (ζ) Potential

The increase in the intensity weighted (z-average) hydrodynamic diameter of ZnO NPs in response to the increase in the electrolyte concentration indicates significant aggregation, especially at 100 mM NaCl (Fig. 2(A)). In contrast to the coated particles, bare ZnO NPs started aggregating at the lowest NaCl concentration of 1mM where the mean intensity weighted hydrodynamic diameters doubled (from 408 ± 83 nm to 816 ± 72 nm (mean ± one standard deviation)). DEX-ZnO NPs were aggregated to some degree even at 0 mM NaCl, at 809 ± 189 nm (mean ± one standard deviation). Negatively charged ZnO NPs (core-shell and DEX(SO_4)) were more resistant to aggregation. At 1 and 10 mM NaCl, negatively charged particle diameters was around 40% and 25% lower than that found with the bare and neutral particles (ZnO and DEX). At the highest electrolyte concentration of 100 mM, all NPs exhibited an increase in aggregation (Fig. 2(A)).

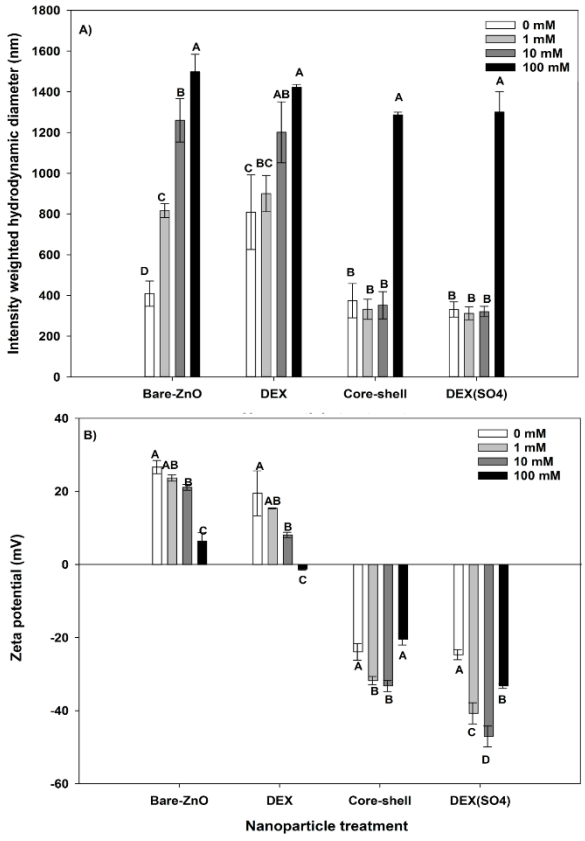

Fig. 2: Effect of NaCl concentration on the hydrodynamic size (A) and Zeta (ζ) potential (B) of ZnO NPs. Treatments connected by different letters at the same ZnO NP treatment are significantly different at α=0.05.

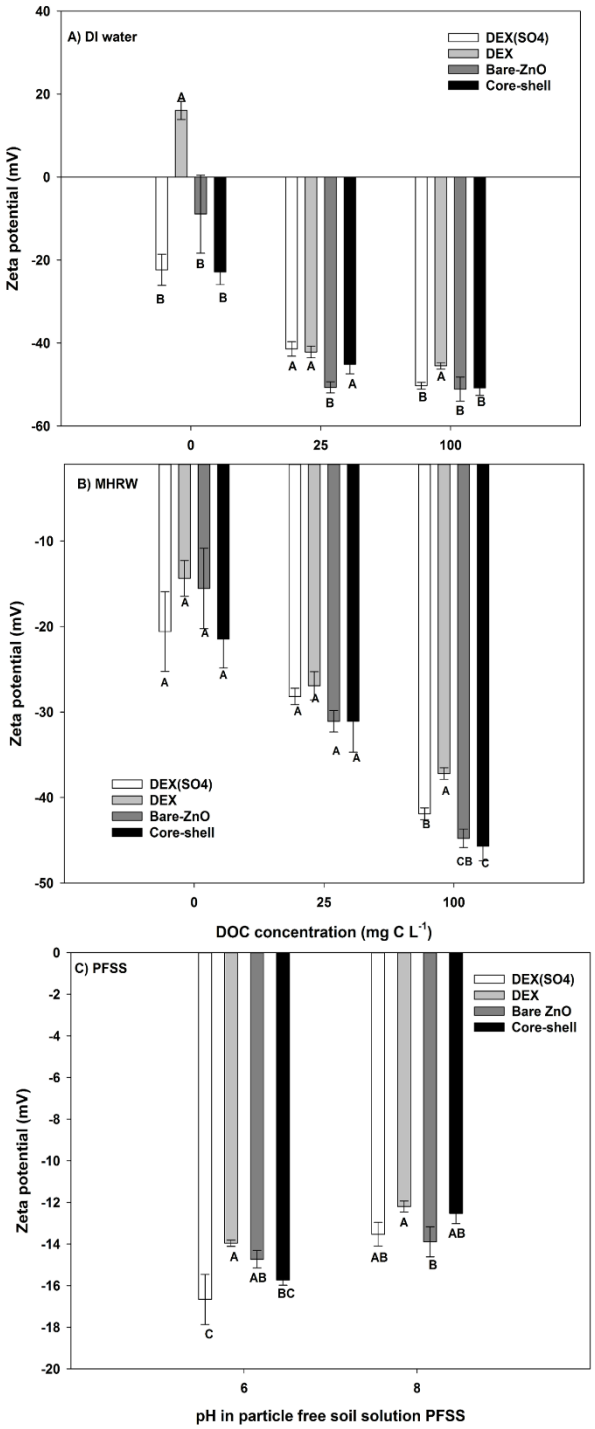

Fig. 3: Zeta (ζ) potential of 25 mg L^{-1} Zn- ZnO NPs suspended in Pahokee peat humic acid -PPHA at 0, 25, and 100 mg C L^{-1} in deionized (DI) water (A), moderately hard reconstituted water (MHRW) (B), and in particle free soil solution (PFSS) (C). Treatments connected by different letters at each PPHA or pH level are significantly different at α=0.05.

The ζ potential values for core-shell and DEX(SO_4)- ZnO NPs remained negative as electrolyte concentration increased (Fig. 2(B)). Whereas for DEX and bare ZnO NPs, ζ potential remained mostly positive (except for DEX at 100 mM NaCl) and significantly

decreased especially when the electrolyte concentration increased to 10 mM. ζ potential values were 0.28 and 0.50 lower for the bare and DEX-ZnO NPs, respectively, in comparison to ζ potential values in DI water. Likewise, at 100 mM NaCl, bare and DEX ZnO NPs had ζ potential values were respectively 4 and 20 times lower than those measured in DI water. For core-shell and DEX(SO_4)-ZnO NPs, increasing the concentration to 1 and 10 mM produced similar ζ potential values which were 1.32 times lower than ζ potential in the absence of the electrolyte. On the other hand, increasing the concentration to 100 mM increased the ζ potential of the core-shell NPs which was not significantly different from the DI treatment (Fig. 2(B)). Zinc oxide NPs coated with dextran sulfate-DEX(SO_4)-followed a similar pattern, albeit more pronounced changes in ζ potential values can be observed. Compared to DI water treatment, ζ potential values for DEX(SO_4)-ZnO NPs were 1.6, 1.9, and 1.3 lower at 1, 10, and 100 mM NaCl, respectively (Fig.2(B)). The pH of all treatments ranged from 7 to 8, so the pH effect on ζ potential was minimal.

Zeta (ζ) Potential of Particles in Simulated Soil Solutions

Increasing DOC concentration in DI tended to lower ζ potential values for all ZnO NPs (Fig. 3(A)). At 0 mg C L^{-1}, only DEX-ZnO NPs exhibited a positive ζ potential (24.1 ± 3.3 mV) (mean ± one standard deviation), while other ZnO NPs had negative ζ potentials and were not significantly different from one another.

When DOC concentration increased to 25 mg C L^{-1}, bare ZnO NPs had significantly lower ζ potential of -50.7 ± 1.34 mV, when compared to the other ZnO NPs, which were not significantly different from one another. The ζ potential for DEX-ZnO NPs at 100 mg C L^{-1} was significantly higher (p = 0.016) than the rest of treatments (-45.5 ± 0.78 mV). It should be noted that we saw different zeta potentials in DI water in figure 2B as compared to figure 3A. This is possibly due to differences in particle dissolution leading to differences in pH and ionic strength.

Likewise, in MHRW, increasing DOC concentration lowered zeta potential of ZnO NPs (Fig.3(B)). There were no significant differences among the NPs at 0 or 25 mg C L^{-1}. However, at 100 mg C L^{-1}, DEX-ZnO NPs had the highest ζ potential (-37.2 ± 0.7 mV) of all treatments (p < 0.05), followed by DEX(SO_4), bare ZnO, and core-shell NPs with ζ potentials of (-41.9 ± 0.7, mV), (-44.8 ± 1.1, mV), and (-45.7 ± 1.7, mV), respectively (mean ± one standard deviation). All ZnO NPs were negatively charged in PFSS, regardless of soil pH (Fig 3.3C). In PFSS at pH6, DEX and DEX(SO_4) ZnO NPs were significantly (p = 0.005) different from one another (-13.99 ± 0.15) vs (-16.67 ± 1.20) mV. Bare ZnO and core shell NPs had similar ζ potential and were not significantly different from DEX or DEX(SO_4) ZnO NPs. At pH8, DEX and bare ZnO NPs had significantly (p = 0.014) different ζ potential values of (-12.20 ± 0.26) and (-13.9 ± 0.72) mV, respectively. Core-shell and DEX(SO_4)-ZnO NPs were not significantly different from each other or from the other two NPs. The increase in carbon concentration in MHRW and DI was accompanied by an increase in the pH values of all ZnO NP suspensions (Table S 1).

Dissolution in Simulated Soil Solutions

Particle free soil solution pH had a tremendous effect on the dissolution of ZnO NPs in the buffered, extracted soil water (Fig.4(A)). Dissolution at pH 6 was higher than at pH8 for all ZnO NP treatments. The nominal total Zn concentration in each treatment was 25 mg L^{-1}. At pH 6, dissolution of core-shell NPs was the lowest with a dissolved Zn concentration of 15.2 ± 0.2 mg Zn L^{-1}. Bare ZnO dissolution (18.6 ± 0.8 mg Zn L^{-1}) was not significantly different from either core-shell NPs or DEX-ZnO NPs (21.9 ± 1.8 mg Zn L^{-1}). Dissolution of DEX(SO_4)-ZnO NPs was the highest (26.2 ± 3.1 mg Zn L^{-1}), which was not significantly different from DEX-ZnO NP. The same trend carried on at pH 8. Core-shell NPs had the lowest dissolution (2.9 ± 0.1 mg Zn L^{-1}), followed by bare ZnO, DEX and DEX(SO_4)-ZnO NPs with dissolution of (3.6 ± 0.3 mg Zn L^{-1}), (4.0 ± 0.1 mg Zn L^{-1}), and (4.4 ± 0.2 mg Zn L^{-1}), respectively (Fig.4(A)).

The DOC concentration also had a big effect on ZnO NP

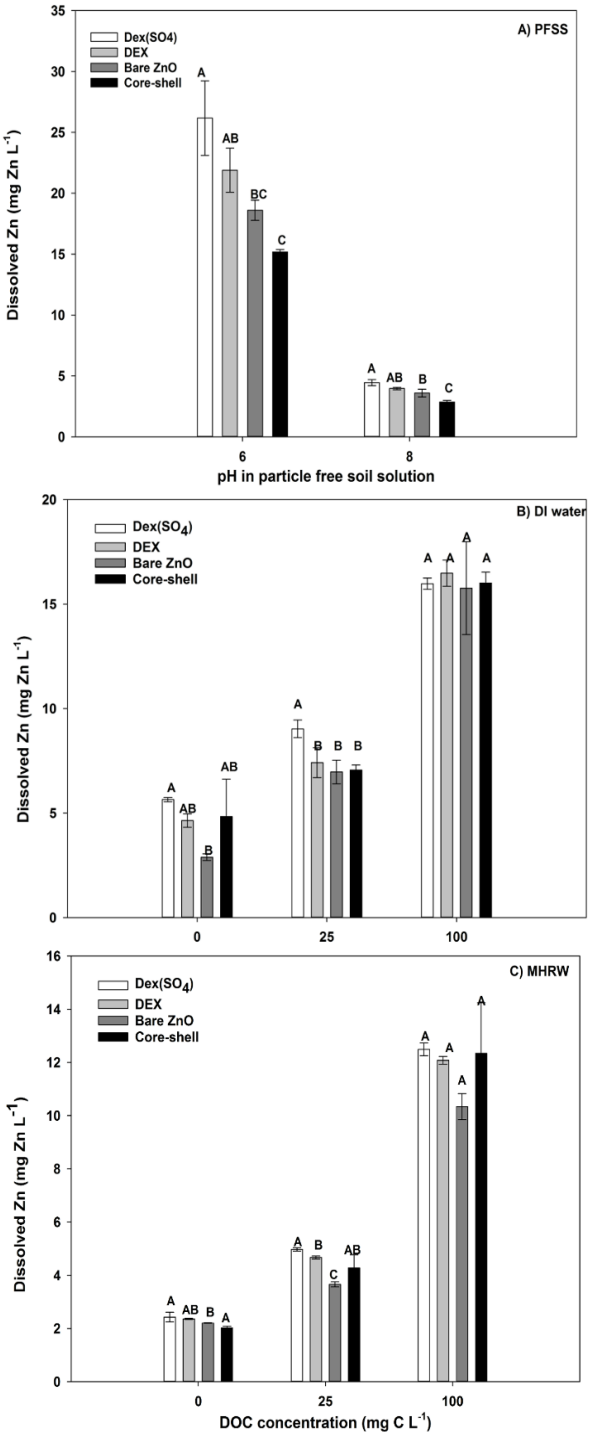

Fig. 4 Dissolution of 25 mg L^{-1} Zn- ZnO NPs in particle free soil solution (PFSS) at pH 6 and 8 (A), in Pahokee peat humic acid (PPHA) solutions at 0, 25, and 100 mg C L^{-1} in deionized (DI) water (B), and in moderately hard reconstituted (MHRW) (C). Treatments connected by different letters at each PPHA or pH level are significantly different at α=0.05.

dissolution. Dissolution of DEX(SO_4)-ZnO NPs in DI water (5.6 ± 0.1 mg Zn L^{-1}) was about twice as great as that for bare ZnO NPs (2.9 ± 0.2 mg Zn L^{-1}) (Fig3.4(B)). The dissolution of DEX(SO_4)-ZnO, DEX-ZnO, and core-shell NPs was the same. Introducing DOC to the ZnO NP suspensions in DI water generally increased the dissolution of the NPs. At 25 mg L^{-1} DOC (1:1 C to Zn mass ratio), DEX(SO_4)-ZnO NPs had the highest dissolution of all ZnO NPs (9.0 ± 0.4 mg Zn L^{-1}). The other ZnO NPs had lower dissolution of around 7.2 mg Zn L^{-1}. Increasing C to Zn ratio 4 times almost doubled the dissolution, from around 6-7 mg Zn L^{-1} at 25 mg L^{-1} DOC to about 16 mg Zn L^{-1}. However, no significant differences were found between ZnO NP treatments (Fig.4(B)).

In MHRW at 0 mg C L^{-1}, core-shell and bare ZnO NPs tended to have lower dissolution, 2.0 and 2.2 mg Zn L^{-1}, whereas DEX and DEX(SO_4)-ZnO NPs both had a dissolution of 2.4 mg Zn L^{-1} (Fig.4(C)). Like DI water, increasing DOC concentration in MHRW significantly increased dissolution; at 25 and 100 mg C L^{-1}, dissolution of ZnO NPs was two and five to six times greater than dissolution in the absence of DOC. When DOC concentration was 25 mg C L^{-1}, bare ZnO NPs had the lowest dissolution of all ZnO NPs (3.7 ± 0.1 mg Zn L^{-1}; $p < 0.05$). Core-shell NP dissolution (4.3 ± 0.5 mg Zn L^{-1}) was significantly lower than that of DEX(SO_4)-ZnO (5.0 ± 0.1 mg Zn L^{-1}). The latter was not significantly different from DEX-ZnO NP dissolution (4.7 ± 0.1 mg Zn L^{-1}). Dissolution was similar (10.3-12.5 mg C L^{-1}) among all ZnO NPs at a DOC concentration of 100 mg C L^{-1} (Fig.4(C)). All NP suspensions experienced a carbon concentration dependent increase in pH (Table S.1).

Natural Organic Matter Sorption

The Freundlich model was fitted to the sorption isotherm of dissolved organic matter to ZnO NPs (Fig.5). All r^2 values suggested that Freundlich isotherm model fitted the data well (Table S 32). The Freundlich constant (k_f) value was similar for most ZnO NPs (0.052-0.054; Table S 2) indicating that similar amounts of PPHA were sorbed at low concentrations. The exception was the core-shell NPs (k_f = 0.041), which sorbed less at low concentrations. The treatments differed in 1/n values (Table S 2), which indicated a difference in the decline in binding as the PPHA concentration increased. Zinc oxide NPs coated with dextran had the highest 1/n value as compared to the rest of the particles with 1/n = 0.577, giving it a more linear sorption isotherm and greater sorption of PPHA at higher concentrations.

On the other hand, DEX-(SO_4)-ZnO had the lowest value (1/n = 0.345) among all treatments, and core-shell and bare ZnO NPs had intermediate 1/n values of 0.515 and 0.433, respectively (Table S 2, Fig.5). The net result was higher sorption of PPHA for DEX-ZnO and bare ZnO NPs as compared to the other treatments at higher PPHA concentrations (> 4 mg L^{-1}).

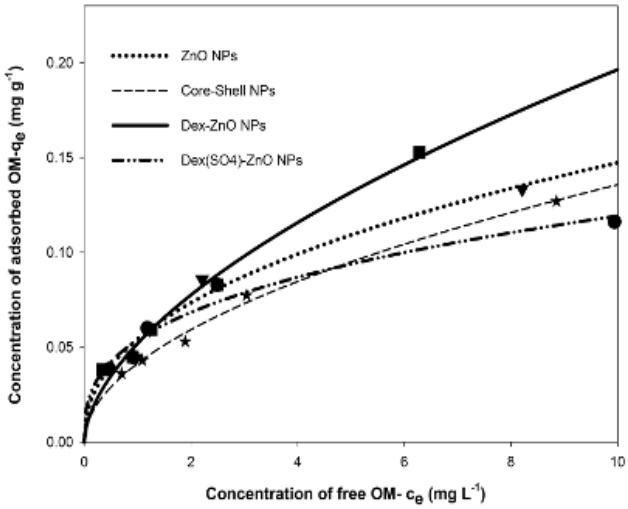

Fig. 5 Freundlich sorption isotherm model fitted to dissolved organic carbon in sorption batch experiments.

Soil and Soil Solution Characterization

Major physiochemical properties of Sadler silt loam are listed (Table 1). Acid leachable, exchangeable, and Mehlich III extractable metals can be found in Table S 3. Major cations and anions, DOC, and ionic strength (IS) for the extracted soil solution for Zn unamended Sadler soil at pH 6 and pH 8 are also listed (Table S 4).

Total Zn Concentration in Soil

Acid leachable Zn recovery of total Zn from the SRM (NIST 2710a, Montana Soil I) was 92.7 ± 2.3% (n=4). The recovery of soil total Zn after saturated paste extraction, as compared to the nominal spiking concentration for $ZnSO_4$, bare, core-shell, DEX- and DEX(SO_4)-ZnO NPs at pH 6 was: 93.1 ± 1.0 %, 92.1 ± 8.5, 94.5 ± 3.0, 87.6 ± 9.8, and 107.2 ± 9.4 %, respectively. Whereas at pH 8, recovered soil Zn was 84.3 ± 4.4, 91.9 ± 7.3, 91.5 ± 13.5, 100.3 ± 11.1, and 85.9 ± 6.9 % for $ZnSO_4$, bare, core-shell, DEX- and DEX(SO_4)-ZnO NPs, respectively. Data presented as (mean ± one standard deviation).

Total and Dissolved Zn Concentration in Soil and Saturated Paste Extracts

For total Zn in soil pore water (Fig.6 (A)), main effects (pH and treatment) were statistically significant (p <0.001, and 0.004, respectively). The treatment by pH interaction was not significant. We performed multiple comparisons between different Zn treatments within each pH level independently. In contrast to $ZnSO_4$, all ZnO NP treatments had significantly increased Zn concentration in the soil solution as compared to the nonamended soil, at both pH 6 and pH 8. When compared to $ZnSO_4$ treated soils at pH 6 (165.1 ± 71.5 µg Zn L^{-1}), total Zn concentrations were increased significantly by factors of 3, 2.6, and 2.4 when soils were

spiked with core-shell (486.1 ± 95.1 µg Zn L^{-1}), DEX-ZnO (422.2 ± 191.4 µg Zn L^{-1}), and bare (401.6 ± 161.2 µg Zn L^{-1}) NPs, respectively. Dextran sulfate coated ZnO NP (376.1 ± 157.4 µg Zn L^{-1}) treatments were not significantly different from $ZnSO_4$ treated soil at pH 6. At pH 8, core-shell (583.9 ± 199 µg Zn L^{-1}) and DEX-ZnO (576.9 ± 218.3 µg Zn L^{-1}) NP treated soils had twice as much total Zn concentration as $ZnSO_4$ at pH 8 (277.3 ± 125.4 µg Zn L^{-1}) (p =*0.05*). Total Zn concentrations for DEX(SO_4) (471.9 ± 37.7 µg Zn L^{-1}) and bare (478.6 ± 149.6 µg Zn L^{-1}) ZnO NP treatments were higher but not significantly different from $ZnSO_4$ at pH 8. None of the nanoparticle ZnO treatments were significantly different from one another in terms of total Zn in soil solution at either pH value (Fig.6(A)).

We also looked at the effects of the ζ potential of ZnO NPs in PFSS on the total Zn concentration in the saturated paste extracts at both pH 6 and 8 (Fig. S4 (A) and (B), respectively). We found that, regardless of soil pH, linear regression between particle ζ potential in PFSS, and total Zn concentration in soil solution was not statistically significant at α=0.05.

Table1 Major physiochemical properties of Sadler soil at unadjusted pH (native pH) and the two adjusted pH levels; 6 and 8

Soil	pH		Particle size distribution			Texture class	OM %	Total N %	CEC cmol kg^{-1}
	DDI	1M KCl	Sand %	Silt %	Clay %				
Native pH	5.54	3.93	9	70	21	Silt loam	1.29	0.13	9.5
pH6	6.19	5.33	NM	NM	NM	NM	NM	NM	NM
pH8	7.4	6.66	NM	NM	NM	NM	NM	NM	NM

NM: Not measured, DDI: Distilled deionized water, OM: Organic matter, CEC: Cation exchange capacity.

For dissolved Zn (Fig. 6(B)), the interaction between Zn treatment and pH was statistically significant (p<0.001). The dissolved Zn concentration for soil spiked with $ZnSO_4$ at pH 6 was 21 times (108.3 ± 67.3 µg Zn L^{-1}) higher than that of the nonamended soil (5.2 ± 3.0 µg Zn L^{-1}) (p < 0.001). Also, $ZnSO_4$ treated soil at pH 6 had significantly higher (7-9 times) dissolved Zn in soil solution as compared to the rest of Zn treatments at pH 6 and about 5.5 times higher than all Zn treatments at pH 8. For pH 8 soil, except for the bare ZnO NPs, all Zn treatments (nano and ionic) were not significantly different from one another. The bare ZnO NP treatment had significantly higher dissolved Zn than the core-shell treatment. Dissolved Zn concentration in soil solution was 40 % higher for ZnO NPs at pH 8 (22.1 ± 5.6 µg Zn L^{-1}) compared to pH 6 (15.8 ± 5.9 µg Zn L^{-1}). At pH 8, DEX-ZnO (21.0 ± 4.7 µg Zn L^{-1}) and bare ZnO NPs treatments had significantly (3 times) higher dissolved Zn in soil solution, as compared to the control (7.3 ± 4.4 µg Zn L^{-1}).

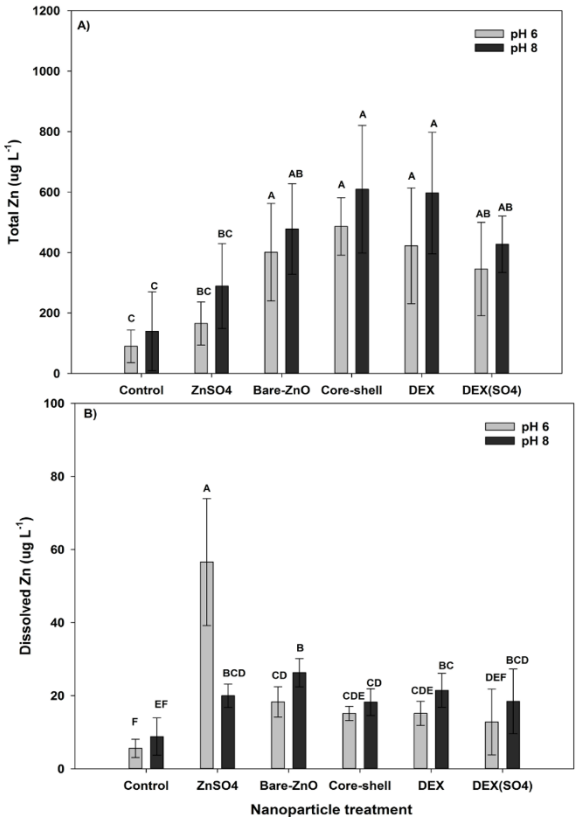

Fig. 6 Total (A) and dissolved (B) Zn concentration in saturated paste extracts. In panel (A), treatments within the same pH level with different letters are significantly different at α=0.05. In panel (B) treatments at both pH levels with different letters are significantly different at α=0.05. Error bars represent ± one standard deviation.

Discussion

In the present study, we aimed to evaluate the effect of surface coatings on the behavior of ZnO NPs in soil at two different pH levels (moderately acidic and alkaline). Our hypothesis stated that, in comparison to positively charged and neutral particles (bare and DEX-ZnO NPs), negatively charged ZnO NPs (core shell-and DEX(SO_4)-ZnO NPs) would have significantly higher partitioning to the soil solution, resulting in an increase in the total Zn concentration in a saturated paste extract. This would be due to the electrostatic repulsion between the negatively charged natural colloids in the soil solution and the negative charge on these NPs, especially at higher soil pH.

The behavior of ZnO NPs in simple aqueous media was mainly dictated by the surface chemistry of the NPs. Negatively charged ZnO NPs (core shell and DEX(SO_4)-ZnO NPs) were more stable against aggregation compared to the neutral DEX-ZnO and the positively charged bare ZnO NPs, especially at the highest concentration of the electrolyte (100 mM), which is comparable to the ionic strength reported in the saturated paste extracts of the Sadler silt loam. It should be noted, however, that soil would contain di- and tri-valent ions that can cause bridging effects. This

would cause greater aggregation in soil at a similar ionic strength when compared to an NaCl solution.

Introducing NOM into the media had a profound effect on the behavior of ZnO NPs and tended to negate the effects of the surface coatings applied during NP synthesis. Although at pH 6 and 8, bare and DEX-ZnO NPs should be positively charged given that their PZC is around 9, all NPs became negatively charged in DI, MHRW, and PFSS, likely due to coating replacement or overcoating with NOM. This behavior is consistent with reports for other kinds of NPs, including bare ZnO NPs(26, 47), gum arabic (GA) coated Ag NPs(48), and bare CuO NPs(49).

In the absence of NOM in DI water and PFSS, core-shell and ZnO NPs exhibited lower dissolution than DEX and DEX(SO_4)-ZnO NPs. This could be due to the low solubility of the $Zn_3(PO_4)_2$ (Ksp = 9 x 10^{-33}) present in the shell structure. There were differences among ZnO NPs in their dissolution at the lower carbon concentration (25 mg C L^{-1}). However, at 100 mg C L^{-1}, which is equivalent to a 1: 4 Zn to DOC mass ratio, all the differences among the ZnO NPs diminished and they all produced similar dissolved Zn concentrations.

The reported concentration dependent increase in pH values of the suspensions as dissolved organic carbon concentration increased is a result of the enhanced dissolution of all ZnO NPs regardless of their as-synthesized coatings. Dissolution of ZnO NPs is well known to raise the pH of the solution due to the consumption of hydrogen ions during the reaction (24, 50).

The sorption isotherm experiments clearly showed that the neutral coating-dextran had the highest binding to NOM at higher NOM concentrations, perhaps due to hydrogen bonding, whereas the negatively charged NPs (DEX(SO_4)- ZnO and core-shell) both had lower binding to the NOM, likely due to the electrostatic repulsion between the coatings and the negatively charged functional groups on the NOM, such as carboxylates.

Most of spiked Zn remained within the soil solid phase (~90%), indicating high retention of Zn to the soil regardless of the Zn form. A relatively small fraction of Zn was partitioned to soil solution as determined by saturated paste extraction. Likewise, retention of >80 % of PVP-Ag NPs (51), multi-walled carbon nanotubes (MWCNT)(52), and CIT-ZnO NPs(53) has been reported.

Total Zn concentration data in the saturated paste extracts showed no differences among NP treatments, even at the higher pH values. This relates to the observation made in aqueous solutions that sorption of NOM conferred a net negative charge to all the NPs, regardless of initial surface chemistry. Our hypothesis still holds true in the sense that negatively charged NPs partitioned more Zn to the soil solution at higher soil pH than at lower soil pH. However, the initial charge of the particles was not as important. Our results are in agreement with Whitley et al, 2013, who found that the prolonged aging of electrostatically stabilized CIT-Ag NPs versus sterically stabilized PVP-Ag NPs yielded the same total Ag concentration in sandy loam soil solution, despite the initial higher partitioning of total Ag from CIT-Ag NPs(54). This was likely due to replacement or over coating of the pristine coatings with NOM, although the exchange or overcoating was faster for CIT coating due to its lower molecular weight as compared to the PVP used in this study(54).

The dissolution pattern in saturated paste extracts was different from that in PFSS. There were no differences in dissolution of ZnO NPs at the two pH levels, 6 and 8. One possible explanation for this discrepancy could be the combined effect of NOM and divalent cations such as Ca^{2+}, which could have facilitated the bridging and subsequent heteroaggregation with clay colloids(55), which may have lowered the surface area and thus the dissolution(24). It is also possible that the soil simply acted as a buffer, removing dissolved Zn ions from solution as they were generated.

Although several studies have been performed to test the effect of soil properties on the concentration of ZnO NPs, versus Zn ions, in soil solution(14, 16, 17, 56), the methods applied for the extraction of NPs from the soil removed a large proportion of Zn in the nanoparticle form that would have formed heteroaggregates(18, 57). Read et al.(13) found differences in soil Zn concentration at soil pH 5.9 and 7.2 only when the spiking concentration exceeded 500 mg Zn kg^{-1} soil, whereas soil Zn concentration was not significantly different at the lower concentrations such as the ones we used in the present study.

Overall, compared to $ZnSO_4$, DEX and core-shell ZnO NPs were able to achieve significantly higher total Zn concentrations in saturated paste extracts, especially at pH 8, but not higher dissolved Zn concentrations. This result suggests that nanoscale fertilizers could be more effective in providing plants with Zn, especially under conditions where conventional fertilizers are of limited efficacy. This suggestion relies on the assumption that Zn from ZnO NPs in suspension is bioavailable to plants. Based on our previous research, we believe that this is likely the case(39, 46). This is likely because suspended particles containing Zn can bind to root surfaces and deliver Zn ions to root cells, not the internalization of intact ZnO particles, for which there is little evidence in the literature. The efficacy of such amendments could be greatly improved by selecting coatings with a high affinity for soil organic matter and could eventually prove to be a successful means of providing the Zn required for plant growth.

Conclusions

Data showed that particle surface chemistry among the different particles dictated the behavior of the ZnO NPs in simple aqueous solutions but that the patterns of behavior in natural soil solution were modified by sorption of natural organic matter (NOM). In saturated paste soil extracts, NOM had an immense effect on the partitioning of the particles to the soil solution regardless of the soil pH (acidic or alkaline). In the experiments which involved humic acids, NOM conferred a net negative charge to all NPs regardless of their as-synthesized coatings. This enhanced their partitioning to and stability in soil solution resulting in an increase in the total Zn concentration in a saturated paste extract. The higher affinity of the dextran coating for NOM explained the relatively high concentrations of total Zn in saturated paste extracts from the DEX-ZnO NPs treatments. Overall, at the very conditions that limit total Zn concentrations in saturated paste extracts for $ZnSO_4$, ZnO nanofertilizers (especially core-shell and DEX-ZnO NPs) had better performance demonstrated by the higher total Zn concentration in soil solution, which in turn would reflect a better bioavailability for crops assuming that the uptake of Zn from nanoparticulate phases is possible as proved by previous work, or that plant roots or associated rhizobacteria can release exudates to solubilize these materials.

Conflicts of interest

"There are no conflicts to declare".

Acknowledgements

The authors thank: Division of Regulatory Services at the University of Kentucky, Lexington, KY, J. Grove., B. Lee, R. Rhodes, R. McCulley, J. Nelson, E. Carlisle, M. Vandiviere, O. Wendroth, J. Walton, and D. Qian. This is a publication of the Kentucky Agricultural Experiment Station. This work is supported by the National Institute of Food and Agriculture, U.S. Department of Agriculture - under 1010358. Support was also provided by the National Science Foundation under CBET- 1530594.

References

1. Rodrigues SM, Demokritou P, Dokoozlian N, Hendren CO, Karn B, Mauter MS, et al. Nanotechnology for sustainable food production: promising opportunities and scientific challenges. Environmental Science: Nano. 2017;4(4):767-81.
2. Prasad T, Sudhakar P, Sreenivasulu Y, Latha P, Munaswamy V, Reddy KR, et al. Effect of nanoscale zinc oxide particles on the germination, growth and yield of peanut. Journal of Plant Nutrition. 2012;35(6):905-27.
3. Subbaiah LV, Prasad TN, Krishna TG, Sudhakar P, Reddy BR, Pradeep T. Novel Effects of Nanoparticulate Delivery of Zinc on Growth, Productivity, and Zinc Biofortification in Maize (Zea mays L.). J Agric Food Chem. 2016;64(19):3778-88.
4. Naseeruddin R, Sumathi V, Prasad T, Sudhakar P, Chandrika V, Ravindra Reddy B. Unprecedented Synergistic Effects of Nanoscale Nutrients on Growth, Productivity of Sweet Sorghum [Sorghum bicolor (L.) Moench], and Nutrient Biofortification. J Agric Food Chem. 2018;66(5):1075-84.
5. Dapkekar A, Deshpande P, Oak MD, Paknikar KM, Rajwade JM. Zinc use efficiency is enhanced in wheat through nanofertilization. Sci Rep. 2018;8(1):6832.
6. Antonious G, Silitonga, M., Tsegaye, T., Unrine, J., Coolong, T., Snyder, J. . Elevated concentrations of trace elements in soil do not necessarily reflect metals available to plants. Journal of Environmental Science and Health. 2013;48(3): .
7. Alloway BJ. Soil factors associated with zinc deficiency in crops and humans. Environ Geochem Health. 2009;31(5): .
8. Evans LJ. Chemistry of metal retention by soils. Environmental Science & Technology. 1989;23(9):1046-56.
9. Schultz MF, Benjamin MM, Ferguson JF. Adsorption and desorption of metals on ferrihydrite: reversibility of the reaction and sorption properties of the regenerated solid. Environmental Science & Technology. 1987;21(9):863-9.
10. Bradl HB. Adsorption of heavy metal ions on soils and soils constituents. J Colloid Interface Sci. 2004;277(1):1-18.
11. Lyklema J. Nomenclature, symbols, definitions and measurements for electrified interfaces in aqueous dispersions of solids (recommendations 1991). Pure and Applied Chemistry. 1991;63(6): .
12. Domingos RF, Rafiei Z, Monteiro CE, Khan MAK, Wilkinson KJ. Agglomeration and dissolution of zinc oxide nanoparticles: role of pH, ionic strength and fulvic acid. Environmental Chemistry. 2013;10(4): .
13. Read DS, Matzke M, Gweon HS, Newbold LK, Heggelund L, Ortiz MD, et al. Soil pH effects on the interactions between dissolved zinc, non-nano- and nano-ZnO with soil bacterial communities. Environ Sci Pollut Res Int. 2016;23(5):4120-8.
14. Waalewijn-Kool PL, Ortiz MD, Lofts S, van Gestel CA. The effect of pH on the toxicity of zinc oxide nanoparticles to Folsomia candida in amended field soil. Environ Toxicol Chem. 2013;32(10):2349-55.
15. Waalewijn-Kool PL, Diez Ortiz M, van Straalen NM, van Gestel CA. Sorption, dissolution and pH determine the long-term equilibration and toxicity of coated and uncoated ZnO nanoparticles in soil. Environ Pollut. 2013;178:59-64.
16. Waalewijn-Kool PL, Rupp S, Lofts S, Svendsen C, van Gestel CA. Effect of soil organic matter content and pH on the toxicity of ZnO nanoparticles to Folsomia candida. Ecotoxicol Environ Saf. 2014;108:9-15.
17. Tourinho PS, van Gestel CA, Lofts S, Soares AM, Loureiro S. Influence of soil pH on the toxicity of zinc oxide nanoparticles to the terrestrial isopod Porcellionides pruinosus. Environ Toxicol Chem. 2013;32(12):2808-15.
18. Wang H, Dong YN, Zhu M, Li X, Keller AA, Wang T, et al. Heteroaggregation of engineered nanoparticles and kaolin clays in aqueous environments. Water Res. 2015;80:130-8.
19. Romero-Freire A, Lofts S, Martin Peinado FJ, van Gestel CA. Effects of aging and soil properties on zinc oxide nanoparticle availability and its ecotoxicological effects to the earthworm Eisenia andrei. Environ Toxicol Chem. 2017;36(1):137-46.
20. Lin S, Cheng Y, Liu J, Wiesner MR. Polymeric coatings on silver nanoparticles hinder autoaggregation but enhance attachment to uncoated surfaces. Langmuir. 2012;28(9):4178-86.
21. Sperling RA, Parak WJ. Surface modification, functionalization and bioconjugation of colloidal inorganic nanoparticles. Philos Trans A Math Phys Eng Sci. 2010;368(1915):1333-83.
22. Collin B, Oostveen E, Tsyusko OV, Unrine JM. Influence of natural organic matter and surface charge on the toxicity and bioaccumulation of functionalized ceria nanoparticles in Caenorhabditis elegans. Environ Sci Technol. 2014;48(2):1280-9.
23. Levard C, Reinsch BC, Michel FM, Oumahi C, Lowry GV, Brown GE. Sulfidation processes of PVP-coated silver nanoparticles in aqueous solution: impact on dissolution rate. Environ Sci Technol. 2011;45(12):5260-6.
24. Bian SW, Mudunkotuwa IA, Rupasinghe T, Grassian VH. Aggregation and dissolution of 4 nm ZnO nanoparticles in aqueous environments: influence of pH, ionic strength, size, and adsorption of humic acid. Langmuir. 2011;27(10):6059-68.
25. Levard C, Hotze EM, Lowry GV, Brown GE, Jr. Environmental transformations of silver nanoparticles: impact on stability and toxicity. Environ Sci Technol. 2012;46(13):6900-14.
26. Mudunkotuwa IA, Rupasinghe T, Wu CM, Grassian VH. Dissolution of ZnO nanoparticles at circumneutral pH: a

study of size effects in the presence and absence of citric acid. Langmuir. 2012;28(1):396-403.
27. Ninham BW. On progress in forces since the DLVO theory. Advances in Colloid and Interface Science. 1999;83(1-3):1-17.
28. Louie SM, Phenrat T, Small MJ, Tilton RD, Lowry GV. Parameter identifiability in application of soft particle electrokinetic theory to determine polymer and polyelectrolyte coating thicknesses on colloids. Langmuir. 2012;28(28):10334-47.
29. Lin S, Wiesner MR. Theoretical investigation on the steric interaction in colloidal deposition. Langmuir. 2012;28(43):15233-45.
30. Rathnayake S, Unrine JM, Judy J, Miller AF, Rao W, Bertsch PM. Multitechnique investigation of the pH dependence of phosphate induced transformations of ZnO nanoparticles. Environ Sci Technol. 2014;48(9):4757-64.
31. Rhoades JD. Soluble salts. Methods of Soil Analysis Part 1- Physical and Mineralogical Methods SSSA Book Series: 5 Soil Science Society of America, Madison, WI. 1996: .
32. EPA. Methods for measuring the acute toxicity of effluents and receiving waters to freshwater and marine organisms,. 4th ed EPA/600/4-90/027F Washington, DC. 1993: .
33. Saito T, Koopal LK, van Riemsdijk WH, Nagasaki S, Tanakat S. Adsorption of humic acid on goethite: isotherms, charge adjustments, and potential profiles. Langmuir. 2004;20(3):689-700.
34. Vermeer AWP, Koopal LK. Adsorption of Humic Acids to Mineral Particles. 2. Polydispersity Effects with Polyelectrolyte Adsorption. Langmuir. 1998;14(15):4210-6.
35. Thomas GW. Soil pH and Soil Salinity. Methods of Soil Analysis Part 1- Physical and Mineralogical Methods SSSA Book Series: 5 Soil Science Society of America, Madison, WI
1996: .
36. Gee GW, Bauder, J.W. Particle-size analysis. Methods of Soil Analysis Part 1- Physical and Mineralogical Methods SSSA Book Series: 5 Soil Science Society of America, Madison, WI. 2002: .
37. Kuo S. Phosphorus. Methods of Soil Analysis Part 3-Chemical Methods SSSA Book Series: 5 Soil Science Society of America, Madison, WI. 1996: .
38. EPA. Method 3052: Microwave assisted acid digestion of siliceous and organically based matrices. United States Environmental Protection Agency, Washington, DC, USA. 1996: .
39. Judy JD, McNear DH, Jr., Chen C, Lewis RW, Tsyusko OV, Bertsch PM, et al. Nanomaterials in Biosolids Inhibit Nodulation, Shift Microbial Community Composition, and Result in Increased Metal Uptake Relative to Bulk/Dissolved Metals. Environ Sci Technol. 2015;49(14):8751-8.
40. Solorzano L. Determination of ammonia in natural waters by the phenolhypochlorite method. Limnology and Oceanography 1969;14(5): .
41. Topp GC, Y.T. Galganov, B.C. Ball, M.R. Carter. Chapter 53. . Soil water desorption curves. . MR Carter (ed) Soil sampling and methods of analysis Canadian Society of Soil Science Lewis Publishers, Boca Raton, FL. 1993.: .
42. Soil and Plant Analysis Council. Chapter 8. Micronutrients (boron, copper, iron, manganese, and zinc). In: Soil analysis handbook of reference methods. Soil and Plant Analysis Council, Inc., CRC Press, Boca Raton, FL. 2000.: .
43. Heil D, Sposito G. Organic matter role in illittic soil colloid flocculation: counter ions and pH. Soil Science Society of America Journal. 1993;57(5): .
44. EPA. Method 3005 A: Acid digestion of waters for total recoverable or dissolved metals for analysis by FLAA or ICP spectroscopy. United States Environmental Protection Agency, Washington, DC, USA. 1996: .
45. EPA. Method 200.8: Determination of trace elements in waters and wastes by inductively coupled plasma-mass spectrometry. .
46. Elhaj Baddar Z, Unrine JM. Functionalized-ZnO-nanoparticle seed treatments to enhance growth and zn content of wheat (Triticum aestivum) seedlings. Journal of Agricultural and Food Chemistry. 2018;66(46):12166-78.
47. Jiang C, Aiken GR, Hsu-Kim H. Effects of Natural Organic Matter Properties on the Dissolution Kinetics of Zinc Oxide Nanoparticles. Environ Sci Technol. 2015;49(19):11476-84.
48. Unrine JM, Colman BP, Bone AJ, Gondikas AP, Matson CW. Biotic and abiotic interactions in aquatic microcosms determine fate and toxicity of Ag nanoparticles. Part 1. Aggregation and dissolution. Environ Sci Technol. 2012;46(13):6915-24.
49. Peng C, Shen C, Zheng S, Yang W, Hu H, Liu J, et al. Transformation of CuO Nanoparticles in the Aquatic Environment: Influence of pH, Electrolytes and Natural Organic Matter. Nanomaterials (Basel). 2017;7(10): .
50. Chowdhury . I HY, Walker. S. Container to characterization: Impacts of metal oxide handling, preparation, and solution chemistry on particle stability. Colloids and Surfaces a-Physicochemical and Engineering Aspects. 2010;368: .
51. Cornelis G, DooletteMadeleine Thomas C, McLaughlin MJ, Kirby JK, Beak DG, Chittleborough D. Retention and Dissolution of Engineered Silver Nanoparticles in Natural Soils. Soil Science Society of America Journal. 2012;76(3): .
52. Kasel D, Bradford SA, Simunek J, Putz T, Vereecken H, Klumpp E. Limited transport of functionalized multi-walled carbon nanotubes in two natural soils. Environ Pollut. 2013;180:152-8.
53. Zhao LJ, Peralta-Videa JR, Hernandez-Viezcas JA, Hong J, Gardea-Torresdey JL. Transport and Retention Behavior of ZnO Nanoparticles in Two Natural Soils: Effect of Surface Coating and Soil Composition. Journal of Nano Research. 2012;17:229-42.
54. Whitley AR, Levard C, Oostveen E, Bertsch PM, Matocha CJ, von der Kammer F, et al. Behavior of Ag nanoparticles in soil: effects of particle surface coating, aging and sewage sludge amendment. Environ Pollut. 2013;182:141-9.
55. Philippe A, Schaumann GE. Interactions of dissolved organic matter with natural and engineered

inorganic colloids: a review. Environ Sci Technol. 2014;48(16):8946-62.
56. Heggelund LR, Diez-Ortiz M, Lofts S, Lahive E, Jurkschat K, Wojnarowicz J, et al. Soil pH effects on the comparative toxicity of dissolved zinc, non-nano and nano ZnO to the earthworm Eisenia fetida. Nanotoxicology. 2014;8(5):559-72.
57. Gupta GS, Senapati VA, Dhawan A, Shanker R. Heteroagglomeration of zinc oxide nanoparticles with clay mineral modulates the bioavailability and toxicity of nanoparticle in Tetrahymena pyriformis. J Colloid Interface Sci. 2017;495:9-18.

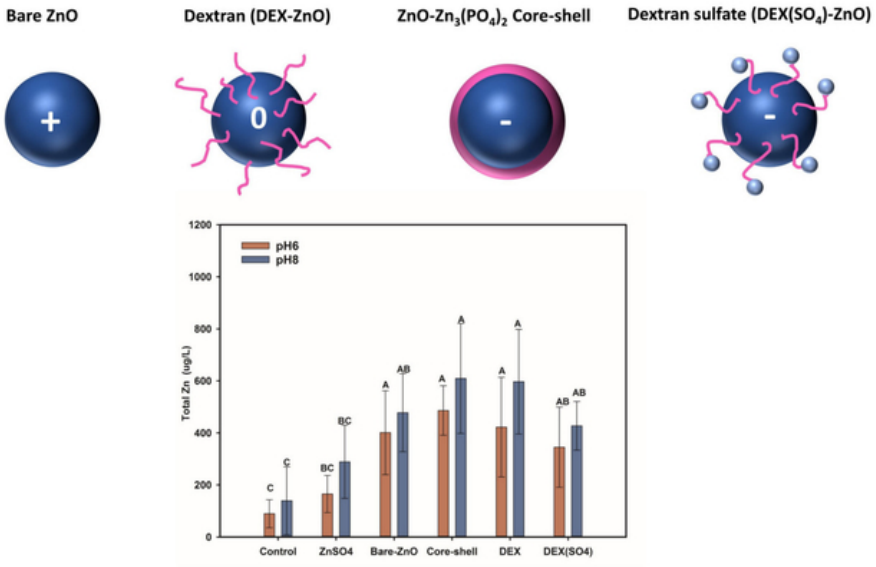

59x34mm (300 x 300 DPI)